VDMA
Fluid Power Association

23rd ISC

International Sealing Conference

Stuttgart, Germany
Sept.30 - Oct.1, 2026

Sealing the future –
Facing the challenges of tomorrow

UNI STUTTGART

Fachverband Fluidtechnik im VDMA e. V. Lyoner Str. 18
50628 Frankfurt am Main
Germany

Phone +49 69 6603-1513
E-Mail maximilian.baxmann@vdma.eu

Internet www.vdma.eu/fluid

Prevention of O-Ring Assembly Damage in ISO 11926 Screw Plugs

Stefan Brödner, Martina Senzel, Manfred Heimann

In the assembly of fluid power sealing systems, reliable and damage-free processes are essential to prevent subsequent leaks. On the one hand, there is a risk of customer complaints and environmental pollution with harmful fluids, and on the other hand, costs increase due to extensive testing, rework or scrap. We observed recurring sealing damages during the screw-in process of screw plugs according to ISO 11926 (UN or UNF threads), fitted with O-rings. At different nominal sizes, the O-rings were consistently cut or squeezed between the bore and the plug. Therefore, we conducted a series of tests, varying several parameters to identify relevant influencing factors concerning geometries, sealing material (rubber type, hardness), and the screw-in process (rotational speed, lubrication). FEA simulations complemented these assembly tests, offering valuable insights into the O-rings' local strain states. Our investigation shows that the O-ring material selection has a decisive influence. Furthermore, we identified potential for improvement through minimal adjustments to the geometry of the screw-in bore. Surprisingly, lubrication in the contact area, typically recommended for seal assembly, proved counterproductive. By combining the findings, the aforementioned problems can be completely eliminated.

1 Introduction

Numerous channels in hydraulic valves, pumps, and cylinders are sealed externally using screw plugs. Depending on their design, these plugs utilize various sealing elements. For designs complying with ISO 11926-2 [1] with a UN/UNF thread according to ISO 725, O-rings are employed. Due to the high-pressure loads acting on these plugs, O-rings made of NBR90 and FKM90 are typically used. These are located between the screw thread and the plug head and are compressed against a 15° cone during assembly, which ensures the tightness of the joint. Owing to the geometry, the O-ring initially contacts the outer radius of the conical surface during the screw-in process (see Figure 1) and must rapidly conform to the installation space.

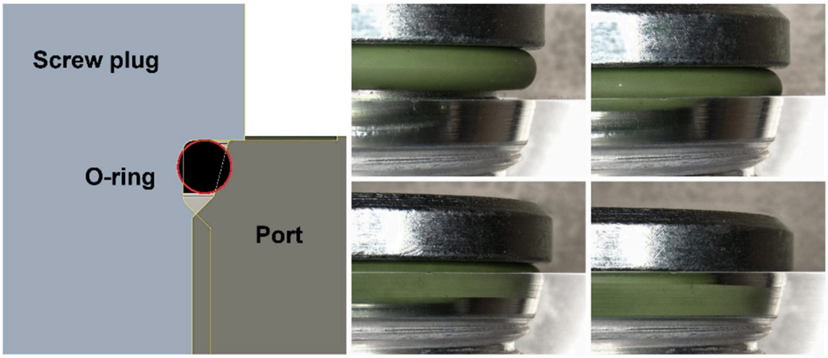

Figure 1: Cross-sectional view of the screw connection (left) and phases of the screw-in process with a transparent housing (right)

Approximately 500.000 screw plugs conforming to ISO 11926 are installed annually across various nominal sizes in hydraulic products at Bosch Rexroth. In recent years, several manufacturing units have observed a rising number of assembly issues during the installation of these plugs. Specifically, significant damage to the O-rings occurs repeatedly. The critical dimensions of the components (plug, O-ring, and port) as well as the surface roughness remain within the permissible tolerance limits. Notably, these failures only occur with FKM90 O-rings. The plugs fitted with NBR90 O-rings can consistently be assembled without damage. Consequently, we conducted extensive assembly tests in which several influencing parameters were varied. These tests were supplemented by a finite element analysis of the assembly process.

All subsequent experimental results were determined for the screw plug size 7/8-14 UNF-2A with the corresponding O-ring size 19,18 x 2,46 mm (AS 568 dash size -910).

2 O-ring Selection and Analysis

Given the apparent influence of the O-ring material, various elastomer compounds were selected for testing: FKM O-rings with a nominal hardness of 70, 80, and 90 IRHD, as well as NBR O-rings with 70 and 90 IRHD.

2.1 Dimensions

The dimensional specifications and tolerances of the O-rings are governed by ISO 11926-2 and -3. All selected O-ring batches were checked on a random basis. Both the inner diameter of 19,18 ±0,13 mm and the cross-section diameter of 2,46 ±0,08 mm were consistently within specifications. The measured values were generally highly congruent with the nominal dimensions.

2.2 Hardness Testing

The durometer hardness (IRHD) of the O-rings was also verified; all specimens were within the specified tolerances.

2.3 Tensile Testing

To gain a better insight into the mechanical behavior of the different elastomer compounds, tensile tests based on ISO 37 were carried out on all O-ring batches. During testing, the O-ring is mounted on two lubricated bolts, which are separated at a constant speed of 200 mm/min until the O-rings breaks.

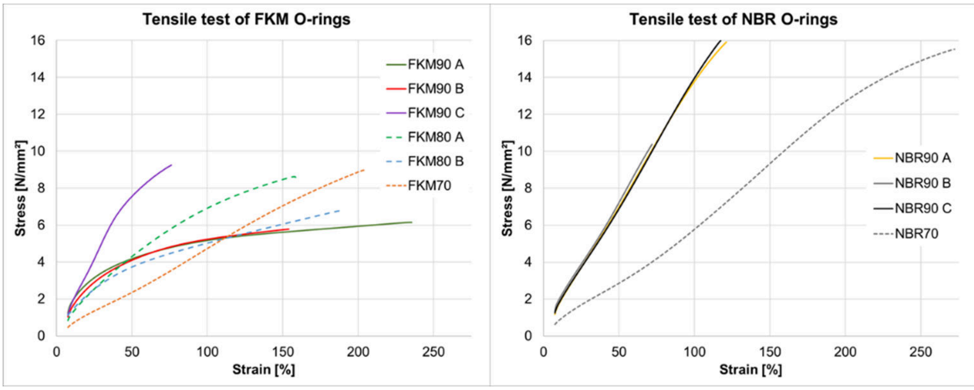

Figure 2: Tensile properties of the investigated O-rings: FKM (left) and NBR (right)

Notably, the stress-strain behavior of several materials does not correlate directly with their durometer hardness (Figure 2). In particular, the tensile curves of most FKM80 and FKM90 O-rings flatten out significantly at strains >30% and fail to reach the stiffness and tensile strength level of the NBR compounds. This suggests that the state of cure (vulcanization) of these O-rings produced in the series production process deviates from that of the standardized test specimens used for establishing their data sheet specifications [2]. The NBR O-rings, on the other hand, exhibit mechanical properties that closely align with the respective data sheets.

3 Screw-in Tests

Figure 3 illustrates the critical geometric parameters for screw connections according to ISO 11926 in size 7/8-14 UNF-2A.

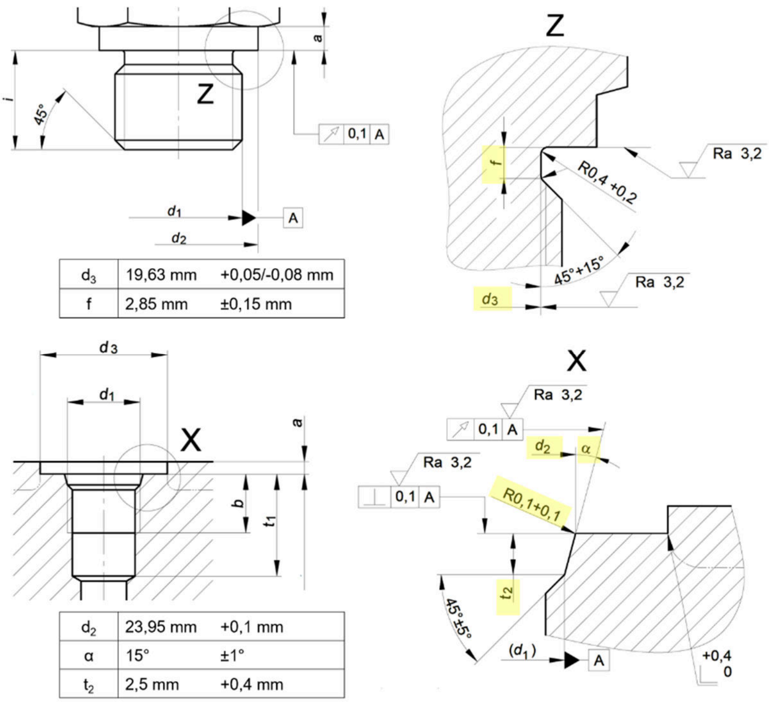

Figure 3: Drawings of the screw-in geometry, size 7/8-14 UNF-2A

3.1 Test Setup

In series production, the screw plugs made of free-cutting steel are assembled into machined connection ports in cast iron housings. For the experimental screw-in tests, ports with slightly varied dimensions were machined. Table 1 outlines the geometry variations evaluated.

Table 1: Variation of the connection port

Port ID	**Diameter d_2 23,95 +0,1 mm**	**Edge radius R 0,1 +0,1 mm**	**Port depth t_2 2,5 +0,4 mm**	**Description**
1	23,95 mm	R 0,10 mm	2,6 mm	Lower limit, series production
2	24,02 mm	R 0,11 mm	2,7 mm	Tolerance center
3	24,11 mm	R 0,10 mm	2,7 mm	Diameter larger than permitted
4	24,01 mm	R 0,30 mm	2,7 mm	Radius larger than permitted
5	23,91 mm	R 0,11 mm	2,7 mm	Diameter smaller than permitted

The screw plugs were sourced from ongoing series production. The most critical parameter is the groove diameter d_3 = 19,63 mm, as this dictates the outer diameter of the mounted O-ring and the subsequent compression. Random sample measurements showed diameters ranging from 19,59 to 19,65 mm.

3.2 O-Ring Installation and Conditioning

The O-ring specimens were mounted onto the production-line screw plugs using a conical assembly sleeve. Due to viscoelastic effects, the O-rings exhibit a temporarily larger inner diameter immediately after the significant stretch during assembly and are initially loose on the screw groove. With increasing storage time, the O-ring shrinks noticeably tighter onto the screw diameter. Microscopic conformability of the elastomer to the rough metal surface further increases the breakaway force over several days. Therefore, a conditioning period of at least one week was maintained after seal assembly before conducting the screw-in tests, ensuring that all O-rings were seated with uniform and comparable firmness.

3.3 Assembly and Process Parameters

The screw-in process depends on numerous factors, most notably assembly speed and lubrication. In series assembly, screwing is typically done mechanically at high rotational speeds of several hundred rpm under dry (unlubricated) conditions.

Variations in rotational speed:

- Approx. 50 rpm (manual assembly)
- Approx. 400 rpm (power tool assembly)

Variations in lubrication state:

- Dry (as-delivered condition)
- Surfaces cleaned (port and O ring)
- Port lubricated only
- O-ring completely lubricated (simulating a coating)

Selected configurations were then screwed in on a dedicated torque-testing rig, allowing precise recording of the required torque at rotational speeds of 25 to 100 rpm.

4 Results

The assembly failures observed in series production were successfully reproduced in our experimental tests. Assembling screw plugs with FKM90 O-rings into connection ports machined with standard production milling tools resulted in highly reproducible damage (Figure 4).

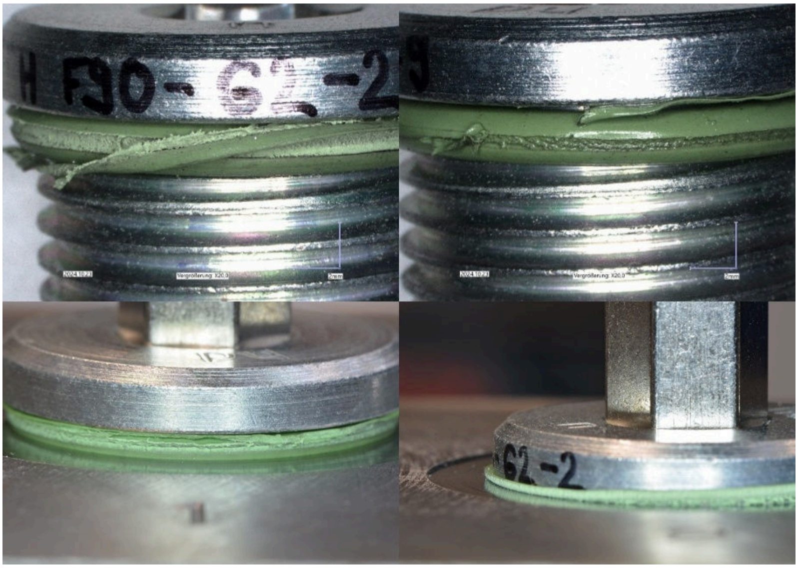

Figure 4: Photographs of damaged FKM90 O-rings (series production conditions)

4.1 Influence of Port Geometry

First, screw plugs with standard production O-rings (FKM90 A) were screwed dry into the tight-tolerance Port 1. The failure rate was substantial, with nearly 50% of the O-rings exhibiting damage (see Figure 5). However, the results with Port 2 (tolerance centre) yielded similarly poor performance. While enlarging the cone diameter (Port 3) had a positive effect, sporadic cutting still occurred. Only with an enlarged edge radius of 0,3 mm (Port 4) was O-ring damage completely eliminated.

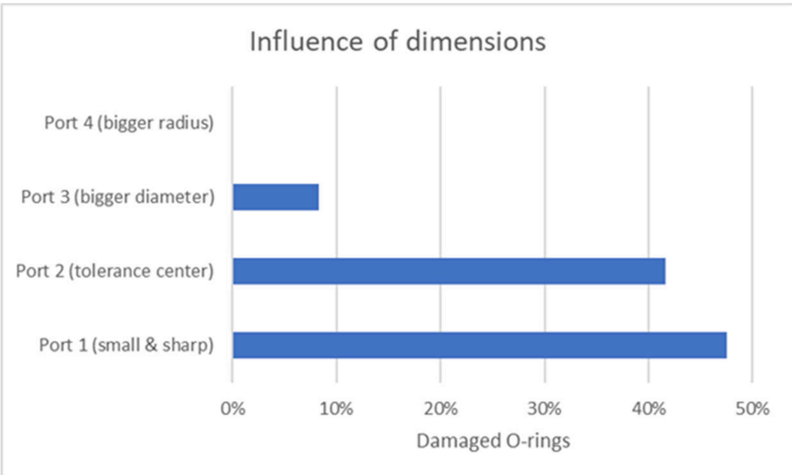

Figure 5: Influence of port geometry on the failure rate of FKM90 O-rings

Torque measurements on the test rig confirm these observations. Figure 6 plots the assembly torque versus the rotation angle until the plug head bottoms out against the port (i.e., complete assembly). As soon as the O-ring touches the cone edge (at approx. -360° rotation angle, not shown in the graph), the torque increases steadily due to seal deformation and compression. At a radius of 0,1 mm, the O-ring was severely damaged during assembly, which is evidenced by a local torque drop at approximately -80° rotation angle. In contrast, the torque curve for the 0,3 mm radius remains smooth, and the required torque is significantly lower, resulting in undamaged seals.

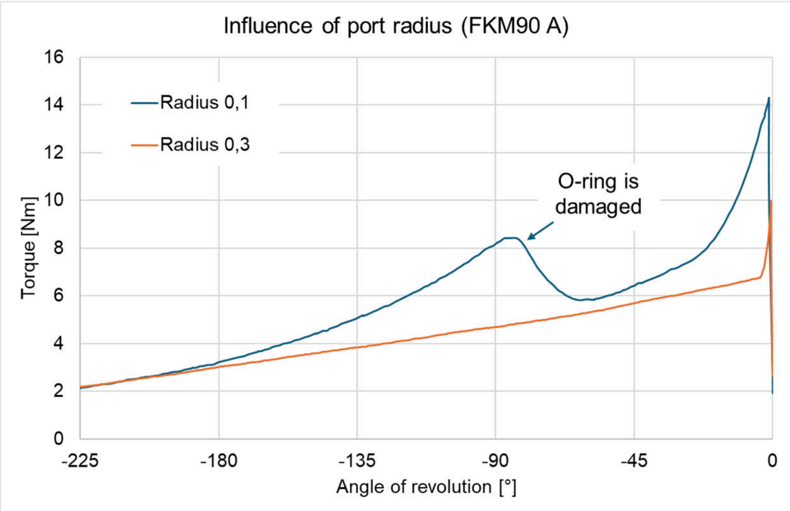

Figure 6: Measured torque curves during assembly for different edge radii (O-ring: FKM90 A, speed: 25 rpm)

4.2 Influence of Assembly Speed

To evaluate process-related factors, standard screw plugs were assembled into Port 1. As illustrated in Figure 7, high failure rates were observed at both low and high rotational speeds. Across all tests, the damage rate was surprisingly higher for slow manual assembly than for rapid mechanical assembly.

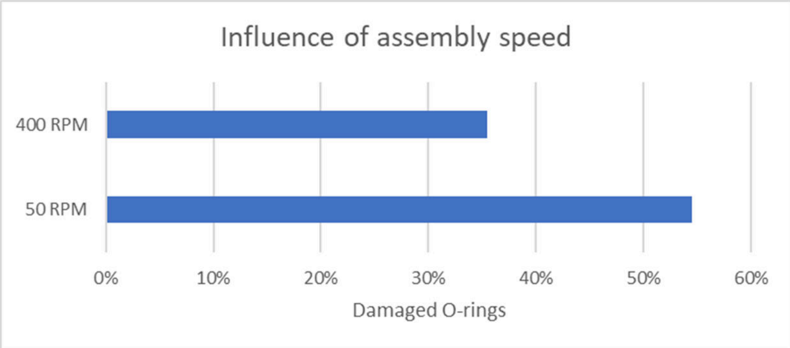

Figure 7: Influence of rotational assembly speed on O-ring damage rate

This trend is also reflected in the torque curves (Figure 8), where a sharp increase in torque occurs regardless of the assembly speed. In all corresponding test runs, the O-rings suffered severe cuts initiated by the sharp port edge.

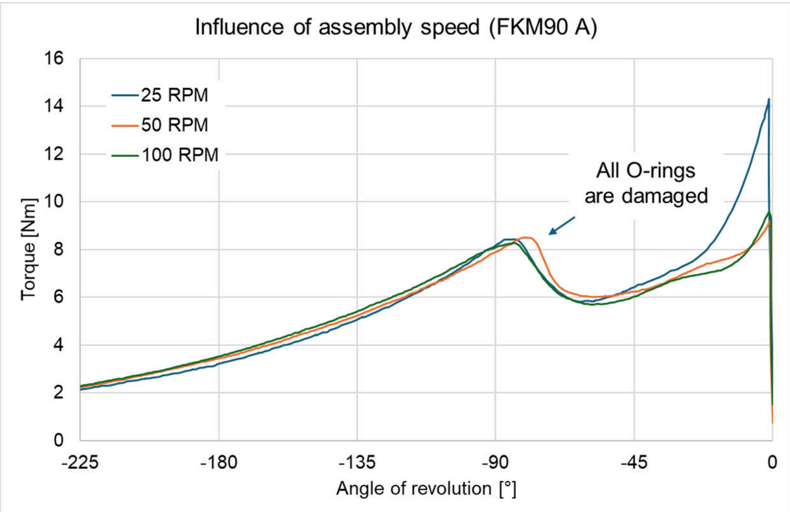

Figure 8: Assembly torque curves at different speeds (O-ring: FKM90 A, Port 1)

4.3 Influence of Lubrication

The lubrication state also revealed surprising results. The common recommendation to lubricate seals during assembly proved only partially effective. When only the port or the outside of the FKM90 O-ring seated on the screw was lubricated, the failure rate actually increased compared to the dry, as-delivered condition. Conversely, cleaning and degreasing the contact surfaces of both the O-ring and the port led to significant improvements (Figure 9). The most reliable assembly was achieved when the O-ring was fully lubricated on all sides (simulating a low-friction surface coating).

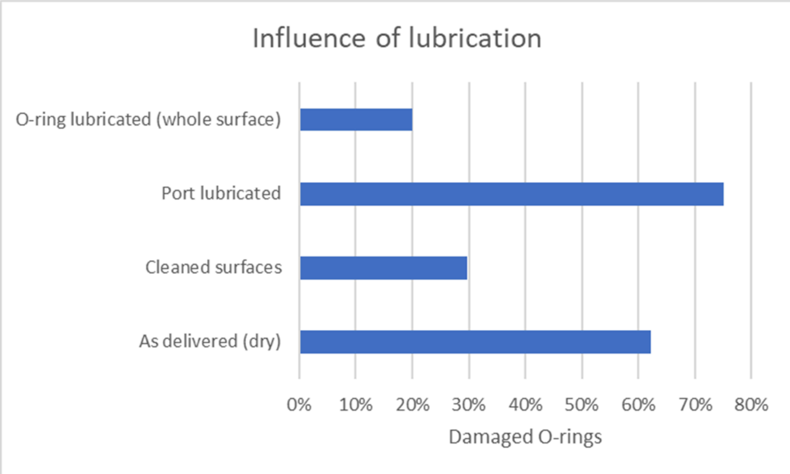

Figure 9: Impact of various lubrication conditions on the failure rate of FKM90 O-rings

Torque measurements on the test rig corroborate these findings, displaying a substantial reduction in assembly torque for fully lubricated or thoroughly cleaned surfaces (Figure 10).

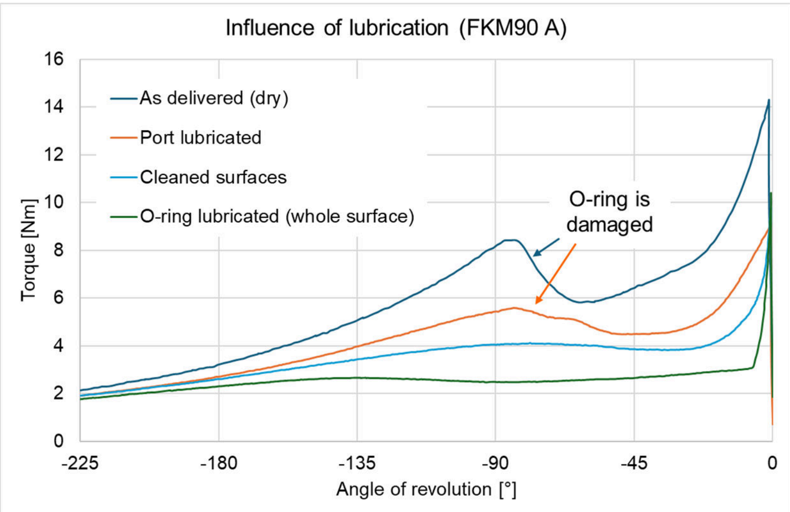

Figure 10: Torque curves under different lubrication conditions (O-ring: FKM90 A, Port 1)

4.4 Influence of O-Ring Compound and Hardness

Finally, the influence of the elastomer compound was systematically evaluated using the critical Port 1. Remarkably, no damage occurred in any of the test runs with the various NBR compounds (70 and 90 IRHD), regardless of the assembly speed or lubrication condition. Even assembly into the undersized Port 5 proceeded without issues.

With the FKM compounds, the performance was strongly dependent on the material hardness and specific formulation. All tested FKM90 compounds suffered extensive damage, with highly consistent failure timing and damage patterns. In contrast, all FKM70 seals were installed without damage – even under the most critical tolerance conditions, behaving similarly to NBR. The FKM80 compounds showed highly inconsistent results: while FKM80 A consistently remained undamaged (even in Port 5), FKM80 B was frequently cut, showing only a minor improvement over the FKM90 materials. Torque measurements highlight these distinct material behaviors (Figure 11).

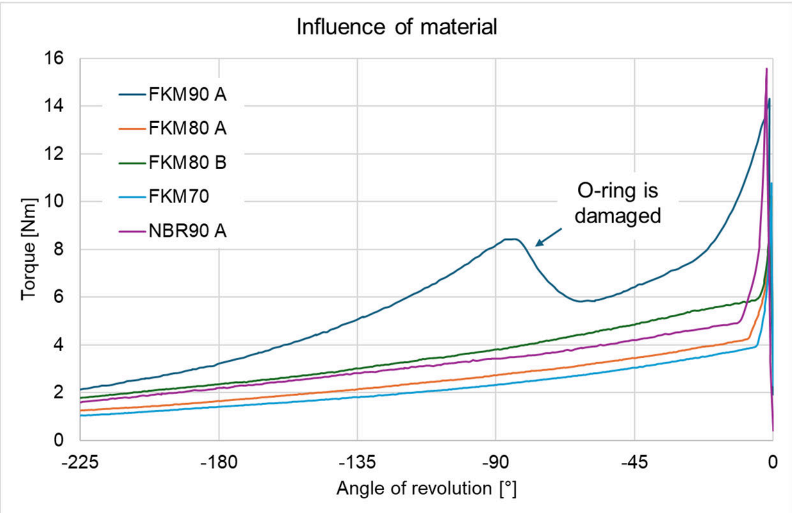

Figure 11: Influence of the elastomer compound and hardness on the assembly torque

4.5 Seal Co-rotation during Assembly

High-speed video analysis of the assembly process revealed a critical kinematic phenomenon: damage to all FKM90 and the FKM80 B O-rings occurred exclusively when the seal was firmly seated on the screw and, despite contact with the port and increasing compression and friction, continued to co-rotate with it. When the O-ring stopped rotating at the port edge while the screw plug slipped and rotated within the seal, the assembly was invariably damage-free. With the other materials, co-rotation could also be observed in some cases, yet no damage ever occurred here. We therefore assume that a combination of the specific material behavior of hard FKM materials together with the cutting effect at the cone edge leads to the frequent damage. Mitigating either factor significantly lowers the failure probability.

5 Finite Element Analysis

In parallel with the experimental testing, a finite element model was developed to simulate the assembly process. To ensure computational efficiency, several simplifications were introduced. Owing to their high structural stiffness, the port and the screw plug were modeled as analytical rigid bodies, while the elastomeric O-ring was represented as a deformable body governed by a hyperelastic Yeoh-Mullins material model. To capture the nearly incompressible behavior of the elastomer, hybrid elements with an additional hydrostatic pressure degree of freedom were utilized for the O-ring mesh. Taking advantage of geometric symmetry, a 2D-axisymmetric model was established. Due to this simplification, the screwing process in the simulation could only be represented as an axial displacement of the screw into the port. Friction at the contact interfaces was represented using Coulomb's friction law. While the actual friction coefficient of unlubricated rubber-to-metal contact can be very high, this typically causes severe convergence issues in implicit FE solvers. After conducting preliminary tests, a constant, global friction coefficient of $\mu = 0{,}25$ was applied.

5.1 Sequence of the Assembly Process

Initially, geometric interferences between the O-ring and the plug groove are resolved in a preliminary step, causing a slight radial stretch of the seal (Figure 12). The port then translates axially upward, bringing the O-ring into contact with the sharp cone edge (Phase I). As displacement continues, the O-ring undergoes progressive deformation and compression (Phase II), forcing itself into the sealing gap until the plug shoulder contacts the port seat (Phase III).

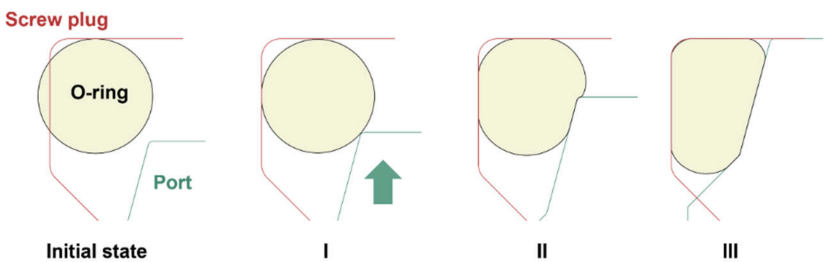

Figure 12: Sequence of the FEM simulation phases

5.2 Influence of the Edge Radius

During the assembly sequence, the elastomer experiences its highest localized deformation directly at the port edge. Coupled with contact friction, this results in severe strain concentrations. Figure 13 displays the nominal principal strains at approximately 65% assembly progress, where the structural load peaks. For an edge radius of 0,1 mm, the maximum local strain reaches approximately 85%, which represents a critical load for many elastomer materials. Increasing the edge radius to 0,2 mm reduces this peak strain to approximately 68%, and a further increase to 0,3 mm lowers it to 63%.

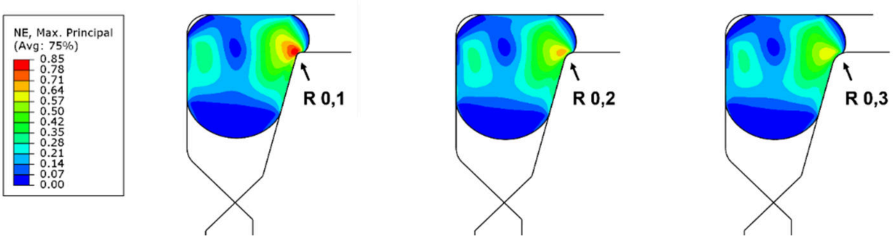

Figure 13: Nominal principal strain at the moment of peak load (0,85 indicates 85% strain)

In addition, the axial reaction forces acting between the screw plug and the port were extracted from the simulation (Figure 14). For the sharpest edge radius (R = 0,1 mm), the force-displacement curve exhibits a local maximum that strongly correlates with the experimental torque curves shown in Figure 6. The O-ring is squeezed on the outside during the axial displacement until it slips a short distance into the cone at approx. 70% progress. In reality, the O-ring was cut at this moment. Increasing the edge radius to 0,2 or 0,3 mm stabilizes the assembly kinetics, yielding a significantly smoother and more continuous reaction force curve.

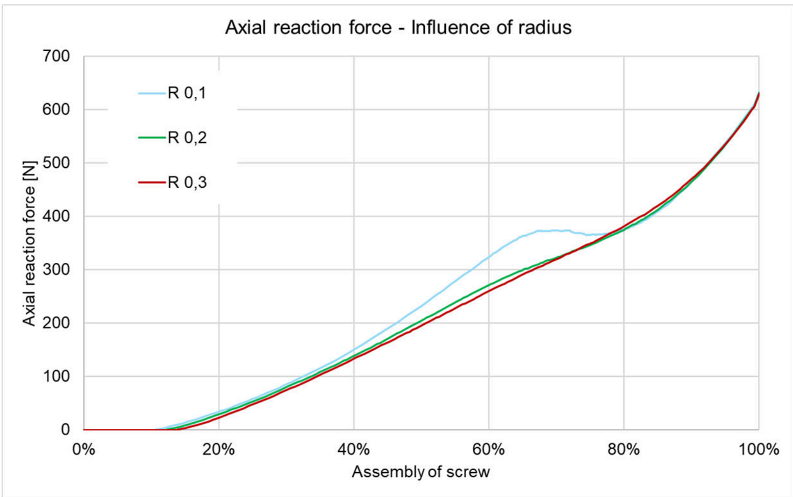

Figure 14: Influence of the edge radius on the axial reaction force during assembly

6 Summary and conclusion

This study systematically investigates recurring assembly damage of O-rings in screw plugs according to ISO 11926 by combining experimental screw-in tests with finite element simulations. The results show that sealing damage is governed by the interaction of elastomer material behavior, local geometry, and assembly conditions. In particular, FKM90 O-rings exhibit a high susceptibility to cutting and squeezing, whereas NBR and softer FKM grades show significantly higher robustness.

A key finding is the critical influence of the connection port geometry. Small edge radii at the cone entrance lead to severe local strain concentrations and promote damage initiation. Increasing the edge radius to 0,3 mm effectively reduces these strain peaks and enables damage-free assembly. Accordingly, the current specification in ISO 11926 should be reconsidered and adapted to an edge radius range of R 0,2 to R 0,3 mm to ensure a robust screw-in process. A slow rotational speed cannot compensate for unfavorable geometry. In addition, lubrication shows a differentiated effect: partial lubrication is detrimental, while either fully clean or fully lubricated conditions improve assembly behavior.

The combined results indicate that damage occurs primarily due to high localized strain at the cone edge in combination with frictional effects and, in critical cases, co-rotation of the O-ring. Hard FKM materials are particularly sensitive to these conditions.

Overall, a reliable and damage-free assembly can be achieved by combining optimized port geometry, suitable material selection, and controlled surface conditions. Implementing these measures enables the elimination of assembly-related sealing damage and improves product quality, manufacturing efficiency, and operational safety.

7 References

[1] ISO 11926-2:1995, Connections for general use and fluid power — Ports and stud ends with ISO 725 threads and O-ring sealing — Part 2: Heavy-duty (S series) stud ends, 1995

[2] Blobner, U., Richter, B.: *Tensile Test on O-Rings – Why and how?*, https://o-ring-prueflabor.de/wp-content/uploads[2024]10/expert_knowledge_-_tensile_test_on_o-rings_06_2019_.pdf, visited on June 12, 2026

8 Authors

Bosch Rexroth AG
Zum Eisengießer 1, 97816 Lohr a. Main, Germany

Stefan Brödner, stefan.broedner@boschrexroth.de

Martina Senzel, martina.senzel@boschrexroth.de

Manfred Heimann, manfred.heimann@boschrexroth.de

https://doi.org/10.61319/ZJQR9GX7